Neural network approach to modeling hot intrusion process for micromold fabrication

Shiu, Pun Pang; Knopf, George K.; Ostojic, Mile; Nikumb, Suwas

Publisher's version / Version de l'éditeur:
https://doi.org/10.1117/12.817359
Optomechatronic Technologies 2008, Proceedings of SPIE; no. 7266, 2008-11-17

Neural network approach to modeling hot intrusion process for micromold fabrication

Pun Pang Shiu[a], George K. Knopf[a], Mile Ostojic[b], and Suwas Nikumb[b]
[a]Dept. of Mechanical & Materials Eng., The University of Western Ontario, London, Ontario, Canada
[b]Industrial Materials Institute, National Research Council Canada, London, Ontario, Canada

ABSTRACT

The rapid fabrication of polymeric mold masters by laser micromachining and hot-intrusion permits the low cost manufacture of microfluidic devices with near optical quality surface finishes. A metallic hot intrusion mask with the desired microfeatures is first machined by laser and then used to produce the mold master by pressing the mask onto a polymethylmethacrylate (PMMA) substrate under applied heat and pressure. A thorough understanding of the physical phenomenon is required to produce features with high dimensional accuracy. A neural network approach to modeling the relationship among microchannel height (H), width (W), the intrusion process parameters of pressure and temperature is described in this paper. Experimentally acquired data are used to both train and test the neural network for parameter-selection. Analysis of the preliminary results shows that the modeling methodology can predict suitable parameters within 6% error.

Keywords: microfluidic devices; neural network modeling; micromold fabrication

1. INTRODUCTION

Microfluidic devices, analytical microsystems, and lab-on-a-chip (LOC) technologies have greatly advanced diagnostic medicine in recent years. These microsystems significantly increase the speed of analysis and lower the cost in performing the tests because of the small amount of reagents consumed during analysis. However, these miniature devices must be disposable in order to avoid sample contamination. It is, therefore, necessary to incorporate cost effective methods of volume production for designing and developing microfluidic devices.

The methods of volume production for polymer-based microfluidic devices have been explored previously, such as hot embossing [1,2], and microinjection molding [3,4]. These volume production methods are replication technologies that require mold masters, which are typically expensive to fabricate. The well-recognized methods for fabrication of mold masters of microfluidic devices are the LIGA (lithography, galvano-forming and plastic molding) and Soft-lithography technique. The LIGA method produces microfeatures of mold masters with high quality of surface finishes as well as high aspect ratio structures. The process employed X-ray lithography to transfer microchannel patterns onto PMMA resist. The resulting PMMA microstructures are then electroplated. The limitation of the LIGA method is its high-cost of the process [5,6]. Soft-lithography [7-10] is another popular method to fabricate mold masters. These mold masters are used to replicate polydimethylsiloxane (PDMS) elastomer based microfluidic devices. The microchannel patterns are transferred via UV-lithography technique. The advantage of the method is that UV-lithography systems are widely available. This fabrication method requires a number of steps to produce the mold masters [8]. Both fabrication methods are based on lithography technique.

Shui et al. [11] reported a non-lithography-based method that fabricates metallic mold masters for replication of PDMS-based microfluidic devices. The method involves laser cutting of microchannel features from a thin metallic sheet (50 to 75μm thick) and the microchannel features were then laser welded onto a metal substrate to form the final mold masters. A Y-channel microfluidic mixer fabricated via this method was demonstrated [11]. The advantages of this method to fabricate mold masters are that it only involves a few fabrication steps, laser cutting and welding. The LHEM (Laser micromachining, partial Hot Embossing, and Molding) method is another non-lithography-based mold master fabrication method [12]. The advantage of the method is that the microchannel features of mold masters have near optical surface finishes. The method involves laser micromachining and hot intrusion (partial hot embossing) process. Subsequently, the mold masters were used to replicate PDMS-based microfluidic devices. To design microfludiic

devices using the LHEM method effectively, it is desirable to have a simple model that takes the inputs of desirable dimensions of microchannels and generates the required process parameters. This model could reduce time in designing complex microfluidic networks based on the LHEM method and therefore, increase productivity.

Several researchers have developed models of the hot intrusion process for fabricating polymer microlenses. These researchers [13-15] describe a *contactless intrusion method* in fabrication of microlens array via applying heat and pressure on both the mask and a polymer sheet substrate. Ziolkowski et al. [13] presented a process parameters study on the method and modeled the process using Laplace equation that relates the surface tension and contact angle to estimate the height and radius of the microlenses. Pan et al. [14] demonstrated an experimental and theoretical characterization of micro-embossing process of polymer microlenses fabrication. The optical properties such as focal length of the microlenses and the relative intensity transmitted from the optical fiber were characterized. Shen et al. [15] also presented a similar study of polymeric microlens array via hot intrusion process, which modeled with Arrhenius function. Shiu et al. [16] reported the experimental characterization of the LHEM method, where an empirical equation was derived to describe the hot-intrusion process. This model provides practical guidelines to design the microfluidic networks via the LHEM method.

Since the hot-intrusion process can be viewed as a partial hot embossing (HE), the published studies for modeling the HE process [17-20] are also relevant to this research. N. S. Cameron et al. [17] optimized empirically the process parameters for hot embossing lithography for microfluidic devices. K. F. Lei et al. [18] used contact stress analysis to model hot embossing of PMMA microchannels (2D), and showed that the numerical prediction of wall profiles compare closely with experimental results. Y. Luo et al. [19] employed the viscoelastic model to describe the hot embossing of PMMA microchannels. Finally, M. Worgull et al. [20] employed non-linear transient thermo-viscoelasticity constitutive equations to model the hot embossing process. These researchers frequently used finite element analysis software tool to simulate the process, which required extensive simulation time [19, 20].

Magargle et al. [21] proposed that modeling of the functional components of microfluidic devices could be decomposed into separated functional blocks. Further, these blocks were modeled using artificial neural networks (ANN). Y. Wang et al. [22] reported using ANN to model the functional blocks of microfluidic devices. The examples of these components modeled via ANN are microfluidic injector, mixers, and separator [21-24].

In this paper, an artificial neural network (ANN) approach to model the hot intrusion process of the LHEM method that produces micromold masters for replication of microfluidic devices is presented. The results of this work shows that the process can be modeled using ANN without the in-depth understanding of the underlying physical processes. A brief review of the LHEM method is given in Section 2. Section 3 describes the methods of the artificial neural network modeling of the hot intrusion process. The results of training and simulation of the networks are presented in Section 4. Discussion and concluding remarks are given in Sections 5 and 6.

2. BACKGROUND OF THE LHEM METHOD

Fig. 1 illustrates that the fabrication method of a polymethylmethacrylate (PMMA) mold master by the LHEM method. It involves only first, fabrication of a hot intrusion mask by laser micromachining the desired microchannel structure in a thin metallic sheet (cut through), second, hot intruding the microchannel structure by pressing the mask onto a Poly(methylmetha-crylate) PMMA substrate. The PMMA substrate with the relief produced in Step 2 is then employed as a mold master for molding the microchannel structure in polydimethylsiloxane (PDMS) elastomer.

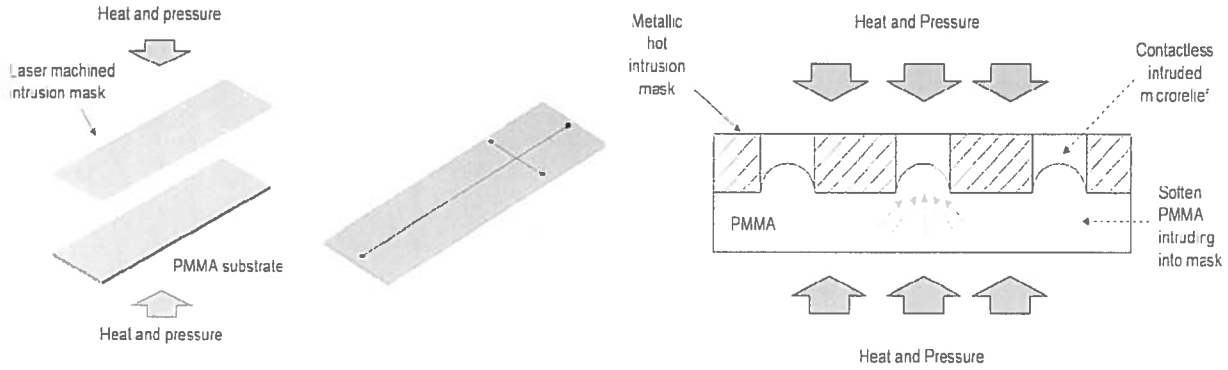

a) Hot intrusion process b) Completed PMMA mold c) Detailed view of hot intrusion

Fig. 1. Rapid fabrication of micromold master via laser cutting and hot-intrusion: a) laser micromachining of the mask and hot intrusion the channel structure onto the PMMA substrate, b) completed PMMA master, c) cross-sectional view of the hot intrusion process in forming the contactless positive microreliefs.

Key advantages of the LHEM method are: simplicity and cost-effectiveness of the process; surface finish of the created microchannel relief is of near optical quality; and a single hot-intrusion mask can be used to produce a large number of mold masters. These properties make the method an attractive option for volume production both in small-and-medium sizes. An SEM view of typical extruded profile of the PMMA mold master of a Capillary Electrophoresis (CE) microfluidic devices fabricated by the LHEM method is shown in Fig. 2 and these typical cross-sectional view is shown in Fig. 3.

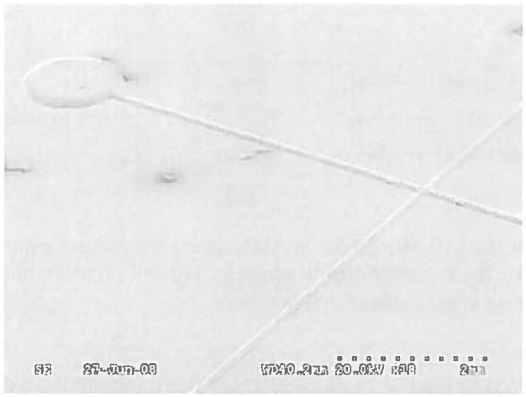

Fig. 2. An SEM view of the Capillary Electrophoresis (CE) micromold master fabricated via LHEM method.

3. FUNCTION APPROXIMATION USING A NEURAL NETWORK

The artificial neural network (ANN) inspired by biological neurons has the ability to approximate non-linear functions [21-25]. For function approximation applications, the neural network structure can involve either supervised or unsupervised training algorithms. The choice depends upon the data and task being solved by the network. In this work, a supervised back-propagation algorithm is used to train the network parameters. The goal is to accurately map multiple inputs to a single output.

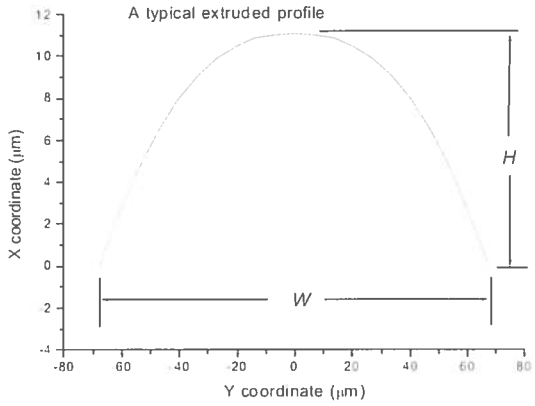

Fig. 3. Typical height (*H*) and width (*W*) of a cross-sectional extruded profile for the micro-relief shown in Fig. 2.

Two neural network models are constructed to model the LHEM process. The first model, Fig. 4a, is referred to as a process model which relates three independent process parameters (hot intrusion pressure, temperature, and width of the profile base) to the height of the extruded microrelief (ie. output).

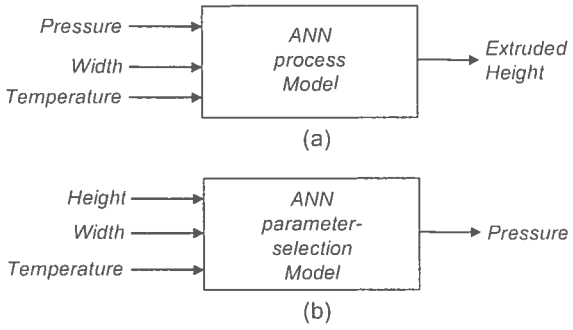

Fig. 4. Neural network models for the LHEM method: a) ANN taking the process parameters and outputs the height of an extruded microrelief, b) taking the desirable profile geometry (*W* and *H*) and outputs the suitable process parameters. The pre-defined static parameter is hot intrusion temperature.

The second model, Fig. 4b, is referred to the *parameter-selection* model which provides the manufacturing engineers and technicians with the ability to relate the desired of the microrelief to a key process variable (pressure). In other words, the parameter-selection model avoids the needs of technicians to understand the physical phenomenon of the process and yet allow the completion of their tasks effectively. The parameter-selection model accepts inputs as the desired microchannel dimensions (width *W*, and height *H* of the extruded profile), and outputs the required process parameters. Although the desired outputs would be hot intrusion pressure and temperature, experimental studies have shown that two different sets of process parameter conditions, mainly different HI pressures and temperatures, can result in similar extruded profiles. Therefore, defining one of the process parameters as a *static parameter* is necessary in order to permit the neural network to generate a single output. In this regard, hot intrusion temperature was selected as the pre-defined static parameter for the parameter-selection model. Furthermore, the hot intrusion time was not taken into consideration because of the experimental results in Shui et al. [16] showed that the influence of hot intrusion time towards the heights of extruded profiles were limited under the experimental condition (2 to 15 minutes). Fig. 5 shows a typical structure of a static backward propagated feed-forward network that was employed in modeling the hot intrusion process of the LHEM method. This type of network is selected for modeling the process because of its computational power in approximating

non-linear functions [25]. The ANN structures used for the tests below were two-layer (n-1) networks for both the process model and parameter-selection model. The training was completed when the network reached the preset mean-square error (MSE) goal.

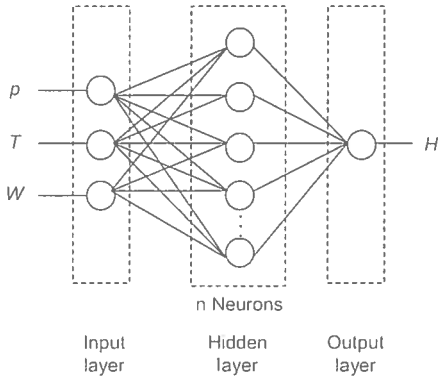

Fig. 5. A two-layer neural network structure for describing the process model of the LHEM method.

To evaluate the performance of the modeling accuracy and identify the appropriate network structure that approximate well the experimental data, the authors tested a number of networks having different n neurons in the hidden layer. The size of the networks was initially large to first obtain a quick convergence solution of the ANN structure. The n number of neurons was then reduced stepwise, tested, simulated, and evaluated the performance. This procedure is stopped when a network structure (n-1) having the fewest neurons possible with small average difference, experimental values minus simulated values.

The mean-square errors (MSE) goal was set at 1×10^{0} for the process model (output in μm) and 1×10^{0} MSE goal for the parameter-selection model (output in Psi). The MSE goal for the process model trained with experimental data was set at one to average out the effects of the possible random errors inherited in the experimental data. The evaluation of ANNs performance was based on the average percentage error between the ANN outputs and the experimental data (all tested networks reached the MSE goal). The number of epochs to reach the goal was set at 10,000. The constructing, training, and testing of the networks were done using the Neural Network ToolBox V. 5.0 from MATLAB, MathWorks, Inc., USA [25].

Both the process and parameter-selection models were trained and tested using the experimental data reported in Shiu et al. [16]. The available experimental data pairs were 45 set (90% of these experimental data were used in training and the remaining 10% data, randomly selected, were used as test set data to evaluate the ANN performance). The process and parameter-selection ANN models hold for the experimental conditions [16] when the pressure ranged from 30 to 60 Psi (207 to 414 kPa), hot intrusion temperature from 110 to 135°C, hot intrusion time from 2 to 15 minutes, extruded profile width from 25 to 200μm, and the processing material is PMMA.

4. RESULTS

Both the process and parameter-selection ANN models were successfully trained using the backward propagation. The optimal ANN structures for the process and parameter-selection models were found. The optimal size of the process model was (7-1) two-layer network structure. The optimal size of parameter-selection model networks was (20-1) because of smaller than that size of networks were not able to reduce to the target MSE for a very long period of time. The approximation of both ANN models was acceptable because the ANN outputs are less than six percent average error against the test data set.

The results of performance evaluation of the ANN process models are showed in Figs. 6 to 8.

Fig. 6 shows that the smallest average percentage difference between the simulated ANN outputs and test set was 3.57% and the smallest average difference was 1.28μm. Figs. 8 and 9 show a comparison between the ANN simulated outputs and experimental data of the optimal network of (7-1). Note that a good approximation of the experimental data by ANN model is clearly shown.

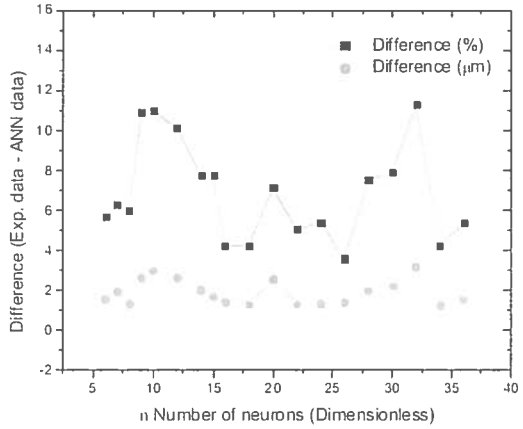

Fig. 6. The differences with n numbers of neurons in the (n-1) of the process model.

Initially, the MSN goals were set as $1x10^{-1}$. After a number of training and testing trials, the resulting ANNs had poor generalization with high degree of undulations. Subsequently, the MSN goal was set as $1x10^{0}$ (MSE 1μm instead of 0.1μm). The generalization was greatly improved. The number of neurons in the networks was further reduced and improved generalization was observed as shown in Fig. 6.

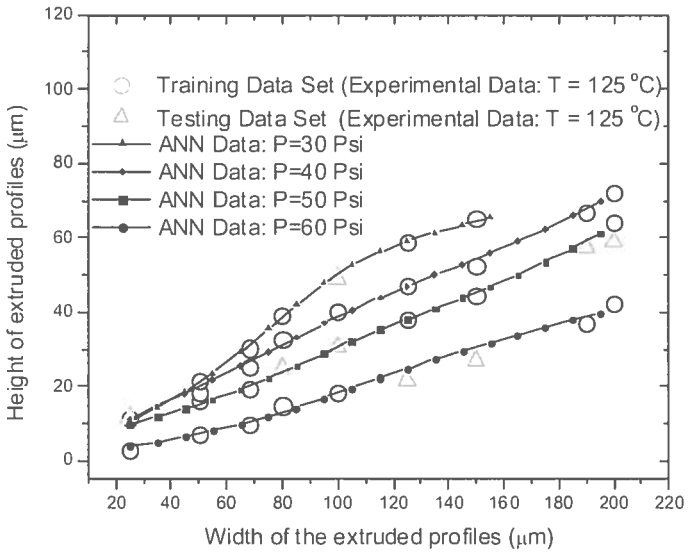

Fig. 7. The outputs of ANN along with experimental data at hot intrusion conditions of 125 °C at 30 Psi to 60 Psi (207 to 414 kPa) of the process model (7-1) ANN structure.

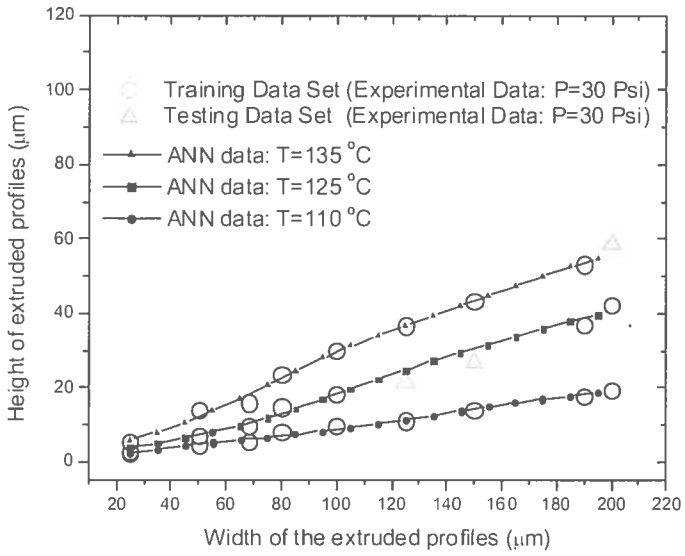

Fig. 8. The outputs of ANN with experimental data at hot intrusion conditions of 110 to 135°C at 30 Psi (207 kPa) of the process model (7-1) ANN structure.

The results of the parameter-selection model are presented below. Fig. 9 describes the results of the percentage error in different n numbers of neurons of two-layer structures. The smallest percentage error of ANN structure is 5.15% and 17.24 kPa (2.5 Psi). Fig. 10 shows that the results of the ANN outputs from the parameter-selection network and demonstrated that the ANN outputs have strong tendency towards 310 kPa (45 Psi) at smaller widths of the extruded profile, less than 70 μm. This tendency can be observed in the difference between the ANN output and the experimental data provided in Fig. 10.

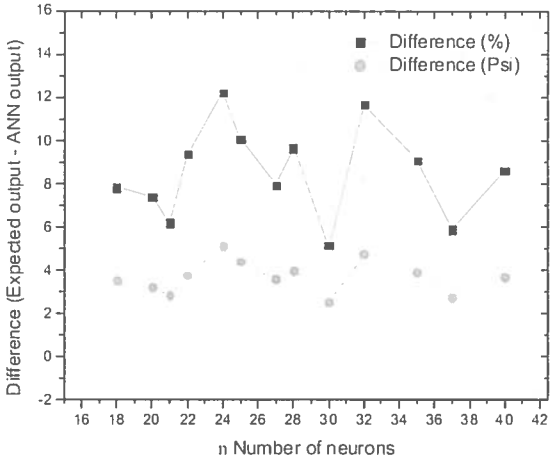

Fig. 9. The differences with n numbers of neurons in the (n-1) of the process model.

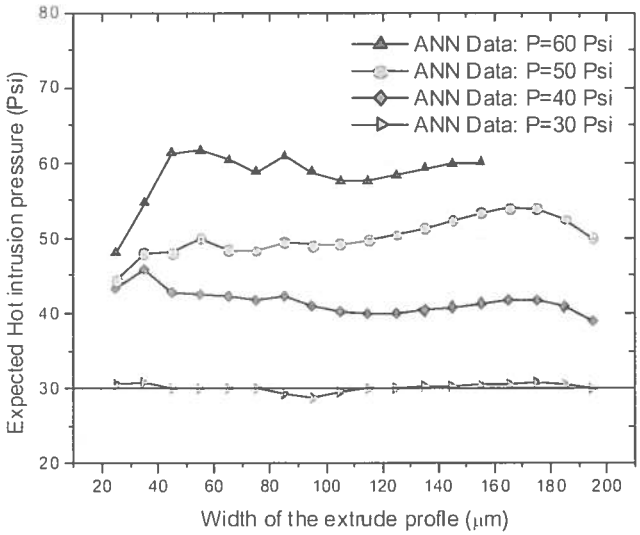

Fig. 10. The comparison of the outputs of ANN and experimental data at hot intrusion conditions of 125°C at 30 Psi to 60 Psi (207 to 414 kPa) of the parameter-selection model (20-1) ANN structure.

Fig. 11 shows the deviation of the simulated outputs from the expected pressure values. At the smaller widths of the extruded profiles, below 70μm, the deviation of the predicted HI pressure values increased. This implies that when designing smaller microreliefs using the parameter-selection ANN model, the resulting microfeatures may have a larger deviation prediction using the trained ANN model.

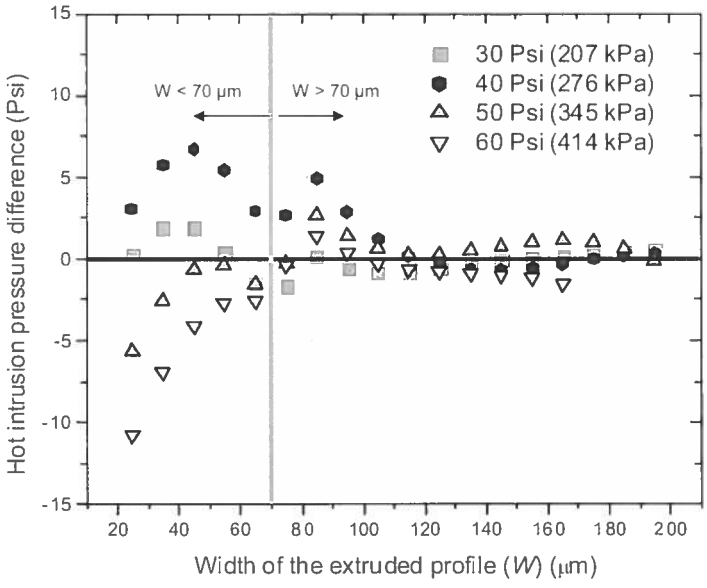

Fig. 11. The deviation of the predicted hot intrusion pressure values vs. width of the extruded profiles, from 30 Psi to 60 Psi (207 to 414 kPa) of the parameter-selection ANN model (20-1) structure.

5. DISCUSSION

The number of neurons of the optimal parameter-selection model was about three times larger than process model's, although the same experimental data were used to train the networks. This shows that the arrangement of the data used in training determines the final number of neurons of the network in this study.

All trained networks reached the target MSE values initially. However, high degree of undulation of the simulated ANN outputs was observed, poor generalizations. Subsequently, the first attempt to minimize the poor generalization was to reduce the number of neurons of the networks because it also reduced the ability of the networks to approximate high order non-linear functions. Poor generalizations of the trained networks were still observed.

The second attempt to minimize the poor generalization of the trained networks was to increase the MSE value. The MSE goal value was set initially to be 1×10^{-1} for process model and it implied that a 0.1μm mean-square-error restricted the network to adapt a lower degree order function to represent to data. MSE goal was adjusted to be 1×10^{0}μm. The networks were re-trained. Subsequently, the generalization was largely improved and further improvement was made by reduced the number of neurons of the networks, shown in Figs. 6 and 9.

The results of the trained parameter-selection model show that some of the simulated ANN outputs (HI pressure values) deviated from the expected values when the input parameter of width of extruded profiles was smaller than 70μm. The contributing factor to this deviation appeared to be that the differences in heights of the extruded profiles are small at smaller widths of extruded profiles, mostly within 5 to 10μm range. The ANN networks may have difficulties to distinguish the difference. However, this problem was not observed in the process model.

If expansion of ANN models is needed for the LHEM method that included different processing material, the modeling approach presented in this paper could be employed. In addition, the trained networks could be incorporated into design/manufacture software (CAD/CAM) to enhance its functionality. For that purpose, portability to different computing devices is necessary; the trained networks could be extracted in a form of analytical equation of simple feed-forward networks of two-layer structure with a single output. The analytical form states as:

$$t_k = y_{out}\left[\sum_{j=0}^{M} g_{kj} z_{hid}\left[\sum_{i=0}^{N} w_{ji} x_i\right]\right], \tag{1}$$

where t_k is the output of the network, $y_{out}[\varsigma]$ is the activation function of linear output, $z_{hid}[\varsigma]$ is the nonlinear activation function of the hidden layer, g_{kj} and w_{ji} are the weights between each neurons.

6. CONCLUSION

In this paper, we presented the artificial neural network (ANN) models that describe the hot intrusion process of the LHEM method. The result showed the ANN models predicted the expected values within 6% difference. Using ANN, we avoided modeling the hot intrusion process via first principles that requires in-depth knowledge of the physical phenomenon, and yet high accuracy of mapping between inputs/outputs was able to achieve. Further, different processing materials used by the LHEM method can be modeled in a similar fashion and portability to different design/manufacture software can be incorporated as well.

ACKNOWLEDGMENT

This paper is a result of the collaboration between the Industrial Materials Institute, National Research Council Canada and The University of Western Ontario, London, Ontario, Canada.

REFERENCES

[1] Becker, H. and Heim, H. "Hot embossing as a method for the fabrication of polymer high aspect ratio structures," Sensors and Actuators A 83, 130-135 (2000).

[2] Heckele, M., Bacher, W. and Muller, K. D. "Hot embossing – the molding technique for plastic microstructures," Microsyst. Technol. 4, 122-124 (1998).

[3] Piotter, V., Hanemannl, T., Ruprecht, R. and Haußelt, J. "Injection molding and related techniques for fabrication of microstructures," Microsyst. Technol. 4, 129-133 (1997).

[4] Larsson, O., Ohman, O., Billman, A., Lundbladh, L., Lindell, C. and Palmskog, G. "Silicon based replication technology of 3D-microstuctures by conventional CD-injection molding techniques," 9th Int. Conf. on Solid-state Sensors and Actuators 2, 1415-1418 (1997).

[5] Duffy, D.C., McDonald, J.C., Schueller, O.J.A. and Whitesides, G.M. "Rapid prototyping of microfluidic systems in poly(dimethylsiloxane)." Anal. Chem. 70, 4974-4984 (1998).

[6] McDonald, J. C., Duffy, D. C., Anderson, J. R., Chiu, D. T., Wu, H., Schueller, O. J. A. and Whitesides, G. M. "Fabrication of microfluidic systems in poly(di-methylsiloxane) – Review." Electrophoresis 21, 27-40 (2000).

[7] Whitesides, G. M. , Ostuni, E., Takayama, S., Jiang, X. and Ingber, D. E. "Soft lithography in biology and biochemistry," Annual Review of Biomedical Engineering 3, 335-373 (2001).

[8] Becker, H. and Locascio, L. "Review polymer microfluidic devices," Talanta 56, 267-287 (2002).

[9] Nguyen, N. T. and Wereley, S. T. [Fundamentals and Applications of Microfluidics], Artech House, 99, (2002).

[10] Cooper McDonald, J. and Whitesides, G. "Poly(dimethylsiloxane) as a Material for Fabricating Microfluidic Devices," Accounts of Chemical Research 35(7), 491-499 (2002).

[11] Shiu, P. P., Knopf, G. K., Ostojic, M. and Nikumb, S., "Rapid fabrication of micromolds for polymeric microfluidic devices," IEEE 20th Canadian Conf. Elec. Comp. Eng. (CCECE), 8-11 (2007).

[12] Shiu, P. P., Knopf, G. K., Ostojic, M. and Nikumb, S., "Rapid fabrication of tooling for microfluidic devices via laser micromachining and hot embossing," J. Micromech. Microeng. 18(2), 025012 (2008).

[13] Ziolkowski, S., Frese, I., Kasprzak, H. and Kufner, S. "Contactless embossing of microlenses-a parameter study," Opt. Eng. 42(5), 1451-1455 (2003).

[14] Pan, L. W., Shen, X. J. and Lin, L. W. "Microplastic lens array fabricated by a hot intrusion process," J. Microelectromech. 13(6), 1063-1071 (2004).

[15] Shen, X. J., Pan, L. W. and Lin, L. W. "Microplastic embossing process: experimental and theoretical characterizations," Sensors and Actuators A 97, 428-433 (2002).

[16] Shiu, P. P., Ostojic, M. Knopf, G. K. and Nikumb, S., "Rapid fabrication of polymethylmethacrylate micromold masters using a hot intrusion process." unpublished.

[17] Cameron, N. S., Roberge, H., Veres, T., Jakeway S. C. and Crabtree, H. J. "High fidelity, high yield production of microfluidic devices by hot embossing lithography: rheology and stiction," Lab Chip 6, 936–941 (2006).

[18] Lei, K. F., Li, W. J. and Yam, Y. "Effects of contact-stress on hot-embossed PMMA microchannel wall profile," Microsyst. Technol. 11, 353–357 (2005).

[19] Luo, Y., Xu, M., Wang, X. D. and Liu, C. "Finite element analysis of PMMA microfluidic chip based on hot embossing technique," J. Phys.: Conf. Ser. 48, 1102-1106 (2006).

[20] Worgull, M., Heckele, M., Hetu, J. F. and Kabanemik, K. K. "Modeling and optimization of the hot embossing process for micro- and nanocomponent fabrication," J. Microlith. 5(1), 1-13 (2006).

[21] Magrargle, R., Hoburg, J. F. and Mukherjee, T. "Microfluidic Injector Models Based on Artificial Neural Networks," IEEE Trans. Computer-Aided Design Integrated Circuits Syst. 24(2), 378-385 (2006).

[22] Wang, Y., Lin, Q. and Mukherjee, T. "Applications of behavioral modeling and simulation on lab-on-a-chip: Micro-mixer and separation system," Conf. of Behavioral Modeling and Simulation, 8-13 (2004).

[23] Magargle, R., Hoburg, J. F. and Mukherjee, T. "An injector component model for complete microfluidic electrokinetic separation systems," Proc. Nanotechnology Conf. (NanoTech), 77–80 (2004).

[24] Wang, Y., Lin, Q. and Mukherjee, T. "System-oriented dispersion models of general-shaped electrophoresis microchannels," Lab Chip 4(5), 453–463 (2004).

[25] Neural Networks Toolbox, Mathworks Inc., Natick, MA, USA, www.mathworks.com